PHYSICAL REVIEW D **89,** 071502(R) (2014)

Ab initio calculation of finite-temperature charmonium potentials

P. W. M. Evans,[1] C. R. Allton,[1] and J.-I. Skullerud[2]

[1]*Department of Physics, Swansea University, Swansea SA2 8PP, United Kingdom*

[2]*Department of Mathematical Physics, National University of Ireland Maynooth Maynooth, County Kildare, Ireland*

(Received 22 March 2013; published 10 April 2014)

The interquark potential in charmonium states is calculated in both the zero and nonzero temperature phases from a first-principles lattice QCD calculation. Simulations with two dynamical quark flavors are used with temperatures T in the range $0.4T_c \lesssim T \lesssim 1.7T_c$, where T_c is the deconfining temperature. The correlators of point-split operators are analyzed to gain spatial information about the charmonium states. A method introduced by the HAL QCD Collaboration and based on the Schrödinger equation is applied to obtain the interquark potential. We find a clear temperature dependence with the central potential agreeing with the Cornell potential in the confined phase and becoming flatter (more screened) as the temperature increases past the deconfining temperature. This is the first time the interquark potential has been calculated for realistic quarks at finite temperature.

DOI: 10.1103/PhysRevD.89.071502 PACS numbers: 12.39.Pn, 11.10.Wx, 12.38.Gc, 14.40.Pq

I. INTRODUCTION

The quark-gluon plasma (QGP) phase of QCD has been studied extensively both in heavy-ion collision experiments at RHIC [1,2] and the LHC [3] as well as in theoretical calculations. However, a complete understanding of this phase is still some distance away. Experiments are hindered by uncertainties in the phenomenology of the QGP, such as the equation of state, transport properties, and spectral features of hadrons. These quantities are required to model the QGP fireball in heavy-ion collisions as it expands and cools back into the hadronic phase in order that the events in the detectors can be properly interpreted.

One of the quantities of interest is the interquark potential in the QGP phase. A temperature dependent charmonium potential underlies the widely cited J/ψ suppression model of [4]. More recent work on statistical models of charmonium production [5,6] and studies assuming transport models of charmonium production [7,8] lead to alternative interpretations. An analogous suppression has recently been found in bottomonium yields in heavy-ion collisions [9,10].

Theoretical work on the interquark potential at high temperature includes early models [11] and perturbative QCD calculations [12]. Furthermore, there have been some recent nonperturbative (i.e. lattice) QCD studies of interquark potentials which are relevant to the work presented here. These fall into two categories: (i) nonzero temperature studies of the static quark potential [13–17] and (ii) zero temperature studies of the potential between quarks with finite masses [18]. The work presented here is a study of the interquark potential of charmonium using physical charm quark masses at finite temperature, and it uses two flavors of light dynamical quark. A particular feature of our work is that our lattices are anisotropic, which has the significant advantage that our correlation functions are determined at a large number of temporal points, hence aiding our analysis.

The method we use is based on the HAL QCD Collaboration's calculation of the internucleon potential relevant for nuclear physics that utilizes the Schrödinger equation [19]. In this work we use their "time-dependent" method [20] to determine the real part of the interquark charmonium potential. In our work we do not consider the width of the state and therefore have access to the real part of the potential only. The possible limitations of the underlying assumption, that a nonrelativistic potential description is valid for these temperatures and quark masses, is a separate issue which will not be discussed here.

Our main conclusion is that the charmonium potential as a function of distance is steepest for low temperatures, T, and becomes flatter at large distances as T increases. This work extends our earlier work in [21].

II. TIME-DEPENDENT SCHRÖDINGER EQUATION APPROACH

Following HAL QCD, we determine the potential using their time-dependent method [20]. The first step is to define charmonium point-split operators,

$$J_\Gamma(x;\mathbf{r}) = q(x)\Gamma U(x, x+\mathbf{r})\bar{q}(x+\mathbf{r}), \tag{1}$$

where $\mathbf{r}$ is the displacement [32] between the charm and anticharm quark fields q and $\bar{q}$, x is the space-time point $(\mathbf{x}, \tau)$, and Γ is a Dirac matrix used to generate vector (J/ψ) or pseudoscalar (η_c) channels. $U(x, x+\mathbf{r})$ is the gauge connection between x and $x+\mathbf{r}$. The correlation functions,

$$C_\Gamma(\mathbf{r}, \tau) = \sum_{\mathbf{x}} \langle J_\Gamma(\mathbf{x}, \tau; \mathbf{r}) J_\Gamma^\dagger(0;\mathbf{0})\rangle, \tag{2}$$

of the point-split and local operators can be expressed in the usual spectral representation,

$$C_\Gamma(\mathbf{r},\tau) = \sum_j \frac{\psi_j^*(\mathbf{0})\psi_j(\mathbf{r})}{2E_j}(e^{-E_j\tau} + e^{-E_j(N_\tau-\tau)}), \quad (3)$$

where the sum is over the states j with the same quantum numbers as the operator J_Γ and where $\psi_j(\mathbf{r})$ are the corresponding Nambu Bethe Salpeter (NBS) wavefunctions. N_τ is the number of lattice points in the temporal direction and is related to the temperature by $T = 1/(a_\tau N_\tau)$, where a_τ is the temporal lattice spacing.

Note that so long as the volume is finite, the spectrum of the Hamiltonian is discrete, even at finite temperature, and hence Eq. (3), which is simply an expansion in eigenstates of the Hamiltonian, is universal.

From now on we consider only radially symmetric (S-wave) states. We differentiate Eq. (3) with respect to time and apply the Schrödinger equation, which in Euclidean space-time is

$$\left[-\frac{1}{2\mu}\frac{\partial^2}{\partial r^2} + V_\Gamma(r)\right]\psi_j(r) = E_j\psi_j(r), \quad (4)$$

where μ is the reduced mass of the $c\bar{c}$ system, $\mu = \frac{1}{2}m_c \simeq \frac{1}{4}M_{J/\psi}$. Ignoring the backward moving contribution (we will discuss this in Sec. IV), we obtain

$$\frac{\partial C_\Gamma(r,\tau)}{\partial\tau} = \sum_j\left(\frac{1}{2\mu}\frac{\partial^2}{\partial r^2} - V_\Gamma(r)\right)\frac{\psi_j^*(0)\psi_j(r)}{2E_j}e^{-E_j\tau}$$
$$= \left(\frac{1}{2\mu}\frac{\partial^2}{\partial r^2} - V_\Gamma(r)\right)C_\Gamma(r,\tau). \quad (5)$$

This can be trivially solved for the potential $V_\Gamma(r)$.

Notice that the NBS wave functions, $\psi_j(r)$, are not explicitly required in the above derivation of $V(r)$. However, we note that HAL QCD's original "wave function" method extracts the ground state wave function, $\psi_0(r)$, from a fit to the large time behavior of the correlation function, $C(r,\tau) \to \psi_0(0)\psi_0(r)e^{-E_0\tau}$, and then uses this $\psi_0(r)$ as input into the Schrödinger equation to obtain the potential [18]. HAL QCD's time-dependent method applied here has the distinct advantage that the correlation functions are used directly, without requiring a fit to the asymptotic state.

The S-wave potential can be expressed as

$$V_\Gamma(r) = V_C(r) + \mathbf{s}_1\cdot\mathbf{s}_2 V_S(r), \quad (6)$$

where V_C is the spin-independent (or "central") potential, V_S is the spin-dependent potential, and $\mathbf{s}_{1,2}$ are the spins of the quarks. We have $\mathbf{s}_1\cdot\mathbf{s}_2 = -3/4, 1/4$ for the pseudoscalar and vector channels, respectively.

TABLE I. Lattice parameters used, including spatial and temporal dimension, N_s and N_τ, temperature, and number of configurations, $N_{\rm cfg}$.

N_s	N_τ	T(MeV)	T/T_c	$N_{\rm cfg}$
12	80	90	0.42	250
12	32	230	1.05	1000
12	28	263	1.20	1000
12	24	306	1.40	500
12	20	368	1.68	1000

III. LATTICE PARAMETERS AND CORRELATORS

We performed lattice calculations of QCD with two dynamical flavors of light quark using a Wilson-type action with anisotropy of $\xi = a_s/a_\tau = 6$, $a_s \simeq 0.162$ fm with temporal and spatial lattice spacings of $a_\tau^{-1} \simeq 7.35$ GeV [22,23]. The other lattice parameters are listed in Table I. We note that the range of temperatures is from the confined phase up to $\sim 1.7T_c$, where T_c is the deconfining transition. The charm quark is simulated with the (anisotropic) clover action, and its mass is set by matching the experimental η_c mass at zero temperature.

IV. RESULTS

We applied Eq. (5) to obtain the potential, $V_\Gamma(r)$, for the temperatures listed in Table I for the vector and pseudoscalar channels separately. In Eq. (5), standard symmetric lattice finite differences are used for the spatial and temporal derivatives. Figure 1 shows the central potential obtained for $T/T_c = 0.42$ and 1.68 as a function of the time, τ, appearing in Eq. (5). For each τ value in Fig. 1, we have vertically shifted the data points so that $V_C(r/a_s = 1) \equiv 0$.

As can be seen, there is a good plateau where the potential $V_C(r)$ is stable. The lack of a plateau at small times is presumably due to lattice artifacts caused by contact terms at the source. The upward trend of data points at large times and high temperature corresponds to time values close to the center of the lattice which are contaminated by backward moving states. We have confirmed this interpretation by successfully modeling the effects of these backward moving states.

The central values for the potentials are obtained from $\tau = 6$, 7, 7 ,7 and 24 for $N_T = 20$, 24, 28, 32 and 80, respectively. The resulting V_C and V_S are shown in Figs. 2 and 3. The left-hand error bars are statistical, and the systematic uncertainty of choosing different values of τ to define the potentials is depicted in the right-hand error bars. In Fig. 2 we include the Cornell potential, $V(r) = -\frac{\kappa}{r} + \frac{r}{a^2} + V_0$ with $\kappa = 0.52$ and $a = 2.34$ GeV^{-1} [24], for reference.

Figure 2 is our main result. We see a clear temperature dependence, and in the confined phase, $T = 0.42T_c$, we see

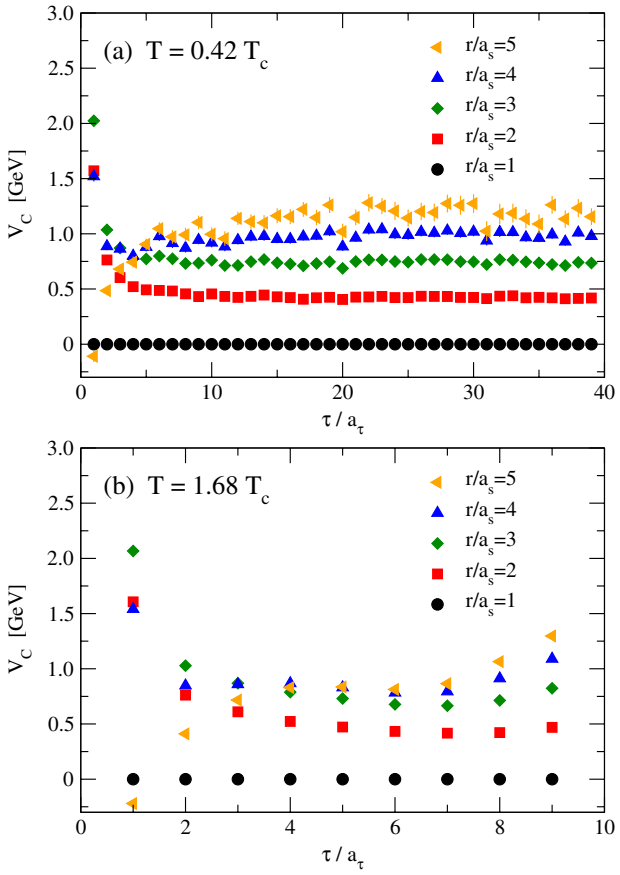

FIG. 1 (color online). The results for the central potential $V_C(r)$ obtained from Eq. (5) for (a) $T = 0.42T_c$ and (b) $1.68T_c$. The horizontal axis is the Euclidean time, τ, appearing in Eq. (5).

evidence of a linearly rising potential in agreement with the Cornell potential. As the temperature increases beyond T_c, the potential flattens for large distances, in agreement with expectations of a deconfined phase. The spin-dependent

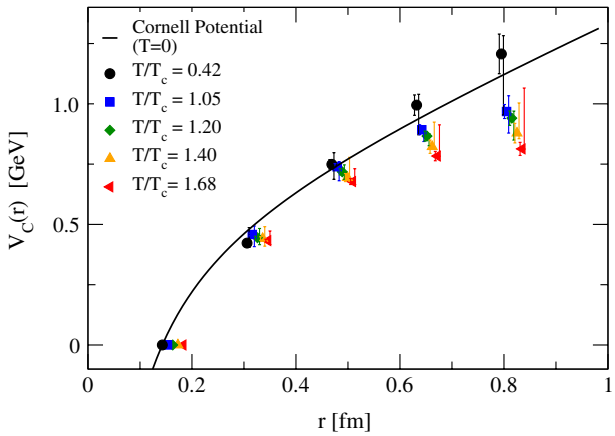

FIG. 2 (color online). Spin-independent (i.e. central) potential, $V_C(r)$, for the temperatures in Table I obtained from Eq. (6). The data points have been shifted horizontally for clarity. The solid curve is the Cornell potential [24] (see text).

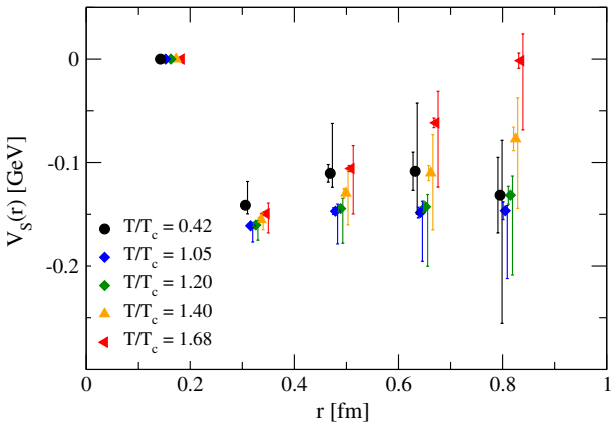

FIG. 3 (color online). Spin-dependent potential, $V_S(r)$, for the temperatures in Table I obtained from Eq. (6), normalized so that $V_S(r/a_2 = 1) \equiv 0$. The data points have been shifted horizontally for clarity.

potential is plotted in Fig. 3 and shows a repulsive core. We plan to improve this calculation by considering relativistic corrections to Eq. (4).

We now compare our results with those using static quarks. There are two general approaches to extract the interquark potential between static (infinitely heavy) quarks, both of which have limitations. The first calculates the free energy of a static quark pair as a function of their separation via various correlators of Polyakov loops [13–15]. However, the "singlet" channel potentials thus derived are gauge dependent [15,25]. Also, it has been argued that the internal energy, or a combination of the free and internal energy, would be a more appropriate definition of the potential at nonzero temperature [26]. The second approach uses Wilson loops or correlators of Wilson lines [15–17] and requires there to be good ground state

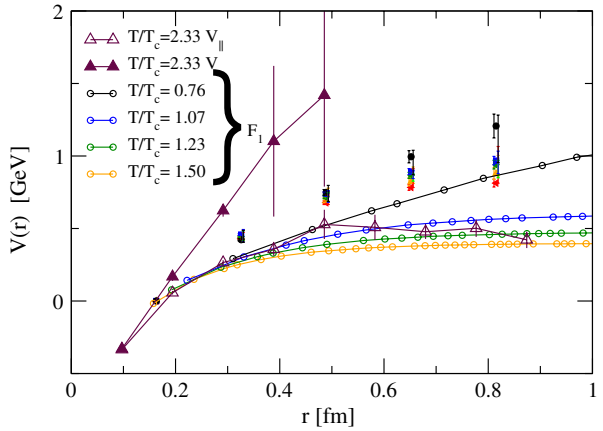

FIG. 4 (color online). Comparison of V_C from this work with the singlet free energy calculation, F_1, from [14] and the Wilson loop, $V_\square$, and Wilson line correlator, $V_\parallel$, from [17]. The error bars of the free energy data are smaller than the symbols. The data from this work follow the legend in Fig. 4.

dominance. However, this creates tension because the temporal extent of the lattice, $N_\tau \sim 1/T$, is necessarily small at high temperature. As a result, precision results are difficult to obtain.

The method discussed here is gauge invariant by construction and produces results with reasonable systematics. Furthermore, it calculates the potential between quarks with finite masses tuned to the physical charm. It does not, however, calculate the imaginary part of the potential, which would require access to the width of the states.

In Fig. 4 we compare our results from Fig. 2 with those obtained from static quark calculations—the singlet free energy [14] and the Wilson loop and line [17]. We note a clear discrepancy between our results and those obtained from static quarks.

V. CONCLUSIONS

There is a significant body of theoretical work studying the interquark potential at nonzero temperature using model, perturbative, and lattice (nonperturbative) approaches. The work outlined here uses a lattice simulation of QCD with two light dynamical flavors on an anisotropic lattice. We determine the charmonium potential at a variety of temperatures using relativistic quarks tuned to the physical charm quark mass. This improves upon earlier lattice simulations performed in the static limit. It thus represents the first *ab initio* calculation of the charmonium potential of QCD at finite temperature.

The method we use is based on the HAL QCD "time-dependent" approach which obtains the real part of the potential from correlators of point-split operators [19]. This allows the extraction of the potential without the need to first define the NBS wave functions by fitting the large time behavior of the correlation functions. This is particularly significant in the nonzero temperature case studied here, where the temporal extent of the lattice is restricted.

Our determination of the potential shows a linearly rising potential for $T < T_c$ in agreement with the Cornell potential, and a clear temperature-dependent flattening of the potential for $T > T_c$. We demonstrate a significant deviation between our results and those obtained using static quarks via either the free energy or Wilson loops/lines.

This work adds to previous charmonium studies performed by our collaboration with the same lattice parameters [23,27] and our earlier work on the potential using the HAL QCD wave function method [21].

In forthcoming work we will simulate on significantly larger lattices with $2 + 1$ light quark flavors. We also hope to extend our work to the potential between heavier quarks using the NRQCD approach [28–30].

ACKNOWLEDGEMENTS

We acknowledge the support and infrastructure provided by the Trinity Centre for High Performance Computing and the IITAC project funded by the HEA under the Program for Research in Third Level Institutes (PRTLI) co-funded by the Irish Government and the European Union. The calculations have been carried out using CHROMA [31]. The work of C. R. A. and P. W. M. E. was carried out as part of the UKQCD Collaboration and the DiRAC Facility jointly funded by STFC, the Large Facilities Capital Fund of BIS and Swansea University. P. W. M. E. and C. R. A. are supported by STFC. C. R. A. thanks the Galileo Galilei Institute for Theoretical Physics for hospitality and the INFN for support during the writing of this work. We are very grateful to Gert Aarts, Sinya Aoki, Robert Edwards, Tetsuo Hatsuda, Balint Joó and Alexander Rothkopf for useful discussions.

[1] J. Adams *et al.* (STAR Collaboration), Nucl. Phys. **A757**, 102 (2005).
[2] K. Adcox *et al.* (PHENIX Collaboration), Nucl. Phys. **A757**, 184 (2005).
[3] K. Aamodt *et al.* (ALICE Collaboration), Eur. Phys. J. C **65**, 111 (2010).
[4] T. Matsui and H. Satz, Phys. Lett. B **178**, 416 (1986).
[5] P. Braun-Munzinger and J. Stachel, Phys. Lett. B **490**, 196 (2000).
[6] P. Braun-Munzinger and J. Stachel, Nucl. Phys. **A690**, 119 (2001).
[7] Y. -P. Liu, Z. Qu, N. Xu, and P.-F. Zhuang, Phys. Lett. B **678**, 72 (2009).
[8] X. Zhao and R. Rapp, Nucl. Phys. **A859**, 114 (2011).
[9] S. Chatrchyan *et al.* (CMS Collaboration), Phys. Rev. Lett. **107**, 052302 (2011).
[10] R. Reed, J. Phys. G **38**, 124185 (2011).
[11] F. Karsch, M. T. Mehr, and H. Satz, Z. Phys. C **37**, 617 (1988).
[12] Y. Burnier, M. Laine, and M. Vepsäläinen, J. High Energy Phys. 01 (2008) 043; N. Brambilla, J. Ghiglieri, A. Vairo, and P. Petreczky, Phys. Rev. D **78**, 014017 (2008); A. Dumitru, Y. Guo, A. Mócsy, and M. Strickland, Phys. Rev. D **79**, 054019 (2009).
[13] O. Kaczmarek, F. Karsch, F. Zantow, and P. Petreczky, Phys. Rev. D **70**, 074505 (2004); **72**059903(E) (2005); Y. Maezawa, N. Ukita, S. Aoki, S. Ejiri, T. Hatsuda, N. Ishii, and K. Kanaya (WHOT-QCD Collaboration), Phys. Rev. D **75**, 074501 (2007); A. Mócsy and P. Petreczky, Phys. Rev.

D **77**, 014501 (2008); Z. Fodor, A. Jakovác, S. D. Katz, and K. K. Szabo, *Proc. Sci.*, LAT2007 (**2007**) 196; P. Petreczky, C. Miao, and A. Mócsy, Nucl. Phys. **A855**, 125 (2011); A. Bazavov and P. Petreczky, Nucl. Phys. **A904–905**, 599c (2013).

[14] O. Kaczmarek and F. Zantow, Phys. Rev. D **71**, 114510 (2005).

[15] A. Bazavov and P. Petreczky, Static quark correlators and quarkonium properties at non-zero temperature, arXiv:1211.5638.

[16] A. Rothkopf, T. Hatsuda, and S. Sasaki, *Proc. Sci.*, LAT2009 (**2009**) 162; A. Rothkopf, T. Hatsuda, and S. Sasaki, Phys. Rev. Lett. **108**, 162001 (2012).

[17] Y. Burnier and A. Rothkopf, Phys. Rev. D **86**, 051503 (2012).

[18] Y. Ikeda and H. Iida, *Proc. Sci.*, LATTICE2010 (**2010**) 143; T. Kawanai and S. Sasaki, Phys. Rev. Lett. **107**, 091601 (2011); Phys. Rev. D **85**, 091503 (2012); *Proc. Sci.*, LATTICE2011 (**2011**) 126; *Proc. Sci.*, LATTICE2011 (**2011**) 195.

[19] N. Ishii, S. Aoki, and T. Hatsuda, Phys. Rev. Lett. **99**, 022001 (2007); S. Aoki, T. Hatsuda, and N. Ishii, Prog. Theor. Phys. **123**, 89 (2010); S. Aoki *et al.* (HAL QCD Collaboration), Prog. Theor. Exp. Phys. **2012**, 01A105 (2012).

[20] N. Ishii (HAL QCD Collaboration), *Proc. Sci.*, LATTICE2011 (**2011**) 160; N. Ishii, S. Aoki, T. Doi, T. Hatsuda, Y. Ikeda, T. Inoue, K. Murano, H. Nemura, and K. Sasaki (HAL QCD Collaboration), Phys. Lett. B **712**, 437 (2012).

[21] C. Allton, W. Evans, and J.-I. Skullerud, *Proc. Sci.*, LATTICE2012 (**2012**) 082.

[22] R. Morrin, A. Ó Cais, M. Peardon, S. M. Ryan, and J.-I. Skullerud, Phys. Rev. D **74**, 014505 (2006).

[23] M. B. Oktay and J.-I. Skullerud, arXiv:1005.1209.

[24] E. Eichten, K. Gottfried, T. Kinoshita, K. D. Lane, and T.-M. Yan, Phys. Rev. D **21**, 203 (1980).

[25] O. Jahn and O. Philipsen, Phys. Rev. D **70**, 074504 (2004); O. Philipsen, Nucl. Phys. **A820**, 33c (2009).

[26] C.-Y. Wong, Phys. Rev. C **72**, 034906 (2005).

[27] G. Aarts, C. Allton, M. B. Oktay, M. Peardon, and J.-I. Skullerud, Phys. Rev. D **76**, 094513 (2007).

[28] G. Aarts, S. Kim, M. P. Lombardo, M. B. Oktay, S. M. Ryan, D. K. Sinclair, and J.-I. Skullerud, Phys. Rev. Lett. **106**, 061602 (2011).

[29] G. Aarts, C. Allton, S. Kim, M. P. Lombardo, M. B. Oktay, S. M. Ryan, D. K. Sinclair, and J. I. Skullerud, J. High Energy Phys. 11 (2011) 103.

[30] G. Aarts, C. Allton, S. Kim, M. P. Lombardo, M. B. Oktay, S. M. Ryan, D. K. Sinclair, and J.-I. Skullerud, J. High Energy Phys. 03 (2013) 084.

[31] R. G. Edwards and B. Joó (SciDAC, LHPC, and UKQCD Collaborations), Nucl. Phys. B, Proc. Suppl. **140**, 832 (2005).

[32] Only on-axis separations were studied in this work.